Sensors and Actuators A 238 (2016) 344–350

Contents lists available at ScienceDirect

Sensors and Actuators A: Physical

journal homepage: www.elsevier.com/locate/sna

Low-humidity sensing properties of diamine- and β-cyclodextrin-functionalized graphene oxide films measured using a quartz-crystal microbalance

Pi-Guey Su*, Yu-Te Lin

Department of Chemistry, Chinese Culture University, Taipei 111, Taiwan

ARTICLE INFO

Article history:
Received 14 September 2015
Received in revised form
14 November 2015
Accepted 23 November 2015
Available online 4 January 2016

Keywords:
Low-humidity sensing
Quartz crystal microbalance
Functionalized graphene oxide
Adsorption dynamic analysis

ABSTRACT

The low-humidity sensing properties of functionalized graphene oxide (GO) thin films with —COOH, —$CONHC_2H_4NH_2$, —$CONH(C_2H_4)_3NH_2$ and β-cyclodextrin (β-CD) functional groups were studied by using a quartz crystal microbalance (QCM). The functionalized GO thin films were characterized by atomic force microscopy (AFM) and Fourier transform infrared spectroscopy (FTIR). Water vapor molecules were easily adsorbed by the functionalized GO thin film with —COOH functional group, but barely adsorbed by the film with the —$CONH(C_2H_4)_3NH_2$ functional group owing to the difference between the difference in the stability of the hydrogen bonds between water molecules and functionalized GO thin films. Adsorption dynamic analysis and molecular mechanical calculations (of the association constant) were performed and the functional groups on the GO were found to affect their humidity-sensing properties (sensitivity), especially at low humidity.

© 2015 Elsevier B.V. All rights reserved.

1. Introduction

Graphene is composed of two-dimensional (2D) arrays of carbon atoms that are covalently connected via sp2 bonds in honeycomb sheets [1]. Graphene has interesting properties, including high electron mobility at room temperature, extraordinary thermal conductivity, superior mechanical properties and low manufacturing cost [2,3]. Graphene oxide (GO) sheets have recently become appealing as potential intermediates in the manufacture of graphene. In GO, carboxyl groups are located at the edges of carbon sheets, whose edges are decorated with epoxy and hydroxyl functional groups [4]. Recently, GO has been widely used as a precursor in the functionalization of graphene because the graphene sheets in GO are heavily oxygenated. The amine group is relatively reactive so both can easily react with various chemicals in the fabrication of amine-functionalized graphene [5,6] and can provide a basis for various sensors [7,8]. In our earlier work [9], an impedance-type relative humidity sensor was fabricated by coating diamine-functionalized GO films on a flexible substrate.

Cyclodextrins (CDs) are cyclic oligosaccharides that are composed of six, seven, or eight glucose units (α, β, or γ-CD, respectively), which are toroidal in shape, and can bind selectively many kinds of organic, inorganic and biological molecules into their cavities to form stable host-guest materials owing to their unique structure [10,11]. Recently, CDs were functionalized to the surface of GO by chemical bonding or strong hydrogen bonding, which is more hydrophilic, favoring the formation of stable CDs-functionalized GO colloidal dispersions for sensing various compounds, such as diethylstilbestrol, dopamine and imidacloprid [11–13].

Consumer demand for reliable and accurate humidity sensors is considerable—especially for use under low-humidity conditions, in meteorological, agricultural, clinical and biotechnological fields [14]. New methods and materials are sought to improve upon existing sensors to detect even lower humidity levels with higher accuracy. Different sensing approaches, including impedance, capacity [15], photonic crystal fiber [16,17], optic [18], field effect transistors (FETs) [19], surface acoustic wave (SAW) [20] and quartz crystal microbalance (QCM) [21–23], have been adopted to detect humidity. QCM is a sensitive mass-measuring device for detecting extremely small changes in mass [24]. Therefore, the QCM-based sensor may represent a promising device for detecting low levels of humidity. Nanosized materials, such as TiO_2 nanowire-based, TiO_2 nanoparticle-based, carbon nanotube (CNT)-based and graphene-based nanomaterials have recently been coated as films on electrodes of quartz crystal microbalance (QCM) to detect low-humidity [25–31]. However, no attempt has been made to fabricate a QCM-based low-

* Corresponding author. Fax: +886 2 28614212.
E-mail addresses: spg@faculty.pccu.edu.tw, spg@ulive.pccu.edu.tw (P.-G. Su).

http://dx.doi.org/10.1016/j.sna.2015.11.034
0924-4247/© 2015 Elsevier B.V. All rights reserved.

www.spm.com.cn

humidity sensor that is based on diamine-functionalized GO and β-CD-functionalized GO films. In this work, ethylenediamine-functionalized GO (EA-GO), 1,6-hexanediamine-functionalized GO (HA-GO) and β-CD-functionalized GO (β-CD-GO) were used to fabricate QCM-based low-humidity sensors. The low-humidity sensing properties of EA-GO, HA-GO and β-CD-GO that were coated on a QCM were compared with those of GO that was coated on a QCM. This study investigates how the functional groups on graphene are related to the low-humidity sensing properties of the graphene-based material, and it emphasizes the most important properties that determine are related to its sensitivity. Furthermore, the dynamics of the adsorption of water vapor molecules onto EA-GO, HA-GO and β-CD-GO thin films that were coated on QCMs and onto the functional groups of GO, themselves, were considered to elucidate the sensing properties of the films.

2. Experimental

2.1. Materials

Graphene oxide (GO; 5 g/L, UniRegion Bio-Tech) were used without further purification. ethylenediamine (98%; EA), 1,6-hexanediamine (98%; HA) *N*-(3-dimethylaminopropyl)-*N*′-ethylcarbodiimide hydrochloride (95%; EDC), *N*-hydroxysuccinimide (95%; NHS), β-cyclodextrin (80 mg/L; β-CD), hydrazine hydrate (N_2H_4) and ammonia (NH_3) were obtained from Aldrich.

2.2. Preparation of EA-GO and HA-GO materials

The preparation of diamine-functionalized GO was similar to that used in our previous study by amidation method [32]. 1 mL of GO (5 g/L) was sonicated in 20 mL DMF for 1 h, and then 0.2 g of EDC and 0.1 g of NHS were added to the GO solution, which was stirred for 2 h at 0 °C. Finally, 12 mmol of EA was added and stirred at room temperature overnight. The product, EA-GO, was separated by filtration and washed three times with acetone and H_2O to ensure that the excess EA was completely removed. Similar synthetic steps were followed to prepare HA-GO.

2.3. Preparation of β-CD-GO material

GO (20 mL, 5 g/L) were mixed with β-CD (20 mL, 80 mg/L). After a brief sonication, the mixture was added to 300 mL ammonia water and 20 μL hydrazine hydrate with strong stirring for 10 min, and the resultant solution was stirred under a water bath at 60 °C for 4 h. Fig. 1 plots the chemical structure of the GO, EA-GO, HA-GO and β-CD-GO.

2.4. Fabrication of QCM electrodes

The AT-cut quartz crystals with a fundamental resonance frequency of 10 MHz and a frequency counter were obtained from ANT Technologies Corp., Taiwan. The surface area of the gold electrode on a QCM was 0.102 cm^2. The gold electrode of the QCM was rinsed in deionized water and then cleaned ultrasonically in acetone. Following drying, both sides of the QCM electrode were coated with the precursor solution by spin coating at a rate of 2000 rpm for 120 s, followed by heating at 60 °C for 15 min in air. Consequently, GO, EA-GO, HA-GO and β-CD-GO thin films had mass values 0.717, 0.739, 1.005 and 0.670 μg, respectively, on the QCM disk. Unless otherwise stated, all measurements were taken at room temperature, around 23.0 ± 1.5 °C.

2.5. Instruments and analysis

As shown in Fig. 2, a divided humidity generator was used as the principal facility for producing the testing gases. The required water vapor concentration was produced by adjusting the proportion of dry and humid air generated by the divided flow humidity generator under a total flow rate is 10 L/min. The model of two mass flow controller's and flow display power-supply used is the Protec PC-540 manufactured by Sierra Instruments Inc. The lowest testing point is limited by the dryness of the gas. A low-humidity hygrometer (HYGROCLIP IC-3, Rotronic Inc.) which measurement range and precision are 0–100% RH and 0.1% RH, respectively, and was used as reference standard hygrometer to measure the testing water vapor concentration produced by the divided flow humidity generator. QCM sensors were connected to an outlet of the divided flow humidity generator and calibrated by the reference standard hygrometer. The setting volume ratio of the moist air and temperature would be adjusted according to the reading of the low-humidity hygrometer calibrated at the CMS/NML (Center for Measurement Standards/National Measurement Laboratory) humidity laboratory. The volume ratio of the moist air was calculated by the following equation:

$$\mathrm{ppm}_v \left(\frac{\mu L}{L}\right) = \frac{V_v}{V} \times 10^6 \quad (1)$$

where V_v is the volume of water vapor and V is the total volume. Measurement procedures were recorded as below: firstly the synthetic dry air was passed through the detection chamber until the deviation of the frequency of QCM was within 2 Hz/s and then the required water vapor concentration was flowed into the detection chamber, finally the synthetic dry air was passed through the detection chamber until the frequency of QCM recovered to its initial value. Sauerbrey [33] first derived the quantitative relationship between changes in frequency Δf (Hz) of the piezoelectric crystal and mass change caused by mass loading on the piezoelectric crystal surface as follows:

$$\Delta f = \left(-2.3 \times 10^{-6} \frac{f_o^2}{A}\right) \Delta m \quad (2)$$

where f_o (MHz) denotes the basic frequency of the unloaded piezoelectric crystal, A (cm^2) represents the surface area of the electrode, and Δm (g) is the change in mass on the crystal surface. The initial volume ratio of the moist air was 2.77 ppm_v for all experiments. All the measurements were performed at the room temperature 23.0 ± 1.5 °C and controlled by the thermostat. The surface microstructure of the thin film that was coated on a QCM was investigated using an atomic force microscope (AFM, Ben-Yuan, CSPM 4000) in tapping mode which the horizontal and vertical resolution are 0.26 and 0.10 nm, respectively. An infrared spectrometer (Nicolet 380) was used to obtain the IR spectra of the diamines-functionalized GO and β-CD-functionalized GO films.

3. Results and discussion

3.1. Surface microstructures of GO, EA-GO, HA-GO and β-CD-GO thin films

The surface morphologies of GO, EA-GO, HA-GO and β-CD-GO films were studied by AFM. Fig. 3 presents the surface topography of 5 μm × 5 μm GO, EA-GO, HA-GO and β-CD-GO films that were coated on QCM electrodes. The root mean square (RMS) roughness values of the GO, EA-GO, HA-GO and β-CD-GO films were 23.1, 25.2, 25.4 and 24.8 nm, respectively. The GO film had a smooth surface with a flake-like and partially wrinkled structure (Fig. 3(a)). The surfaces of EA-GO, HA-GO and β-CD-GO were rougher than that of GO. The values of roughness of EA-GO, HA-GO and β-CD-GO did

www.sim.com.cn

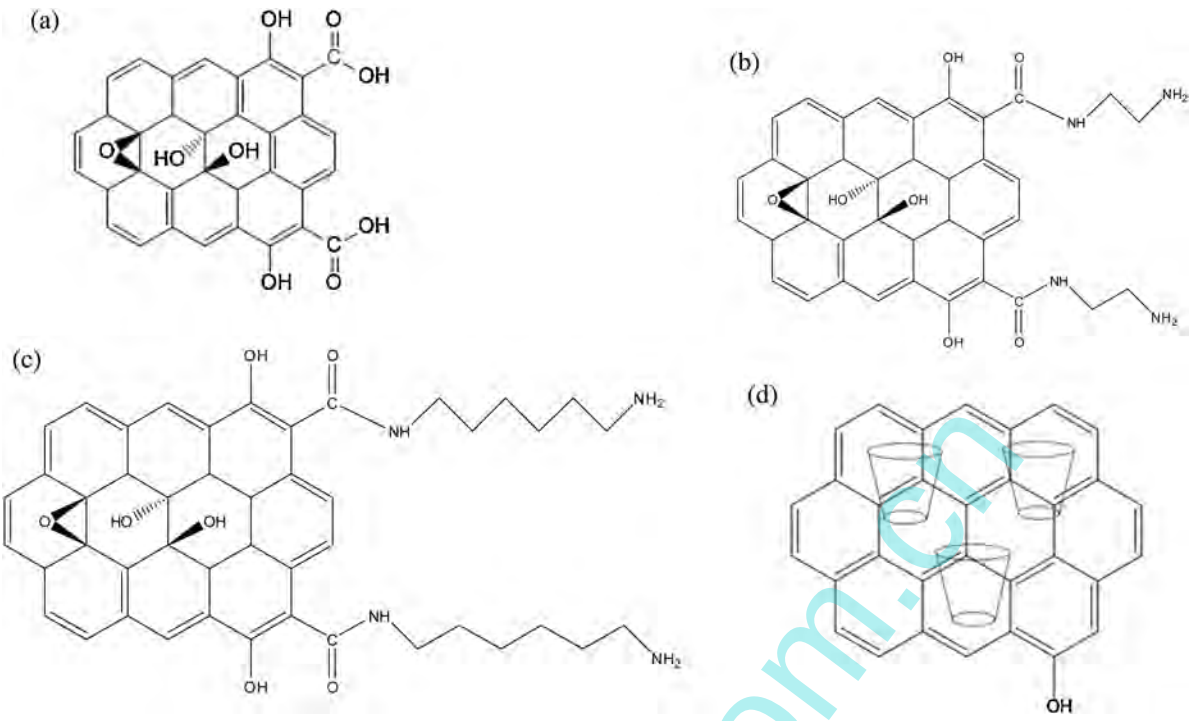

Fig. 1. Chemical structures of (a) GO; (b) EA-GO; (c) HA-GO and (d) β-CD-GO.

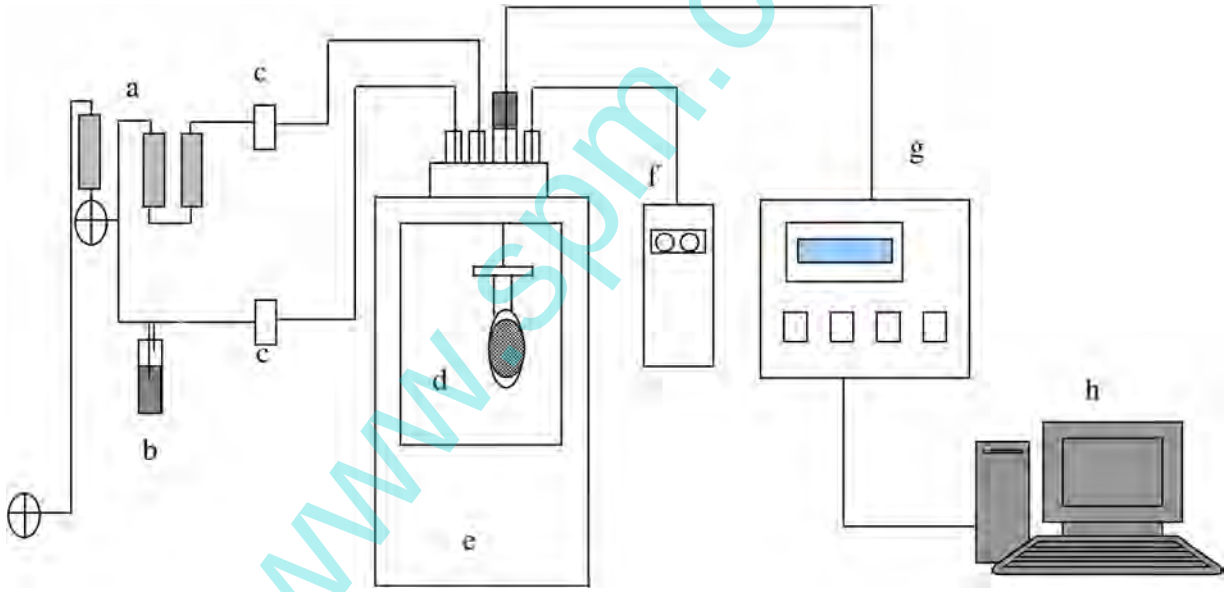

Fig. 2. Schematic diagram of experimental set-up for the QCM sensor measurement and low humidity atmosphere controller. (a) Molecular sieve and desiccating agent; (b) water; (c) mass flow controller; (d) detecting chamber and QCM; (e) thermostat; (f) humidity hygrometer; (g) oscillator and frequency counter; (h) PC.

www.spm.com.cn

not vary significantly (Fig. 3(b–d)). The thickness of EA-GO, HA-GO and β-CD-GO exceeded that of GO.

3.2. IR spectra

GO, EA-GO and β-CD-GO films were investigated by IR spectroscopy. Fig. 4 shows the FT-IR spectra of GO, EA-GO and β-CD-GO, which provides information about the chemical interactions between GO and EA and between GO and β-CD. Typical peaks of GO are observed at 1658 and 1407 cm^{-1}, corresponding to the C=O stretching vibration (COOH group) and the deformation of O—H, respectively. These results reveal that the surface of the graphene was functionalized with carboxyl groups. The EA-GO yielded a peak at 1086 cm^{-1}, which is associated with the C—N stretching of the amide group, and a peak at 787 cm^{-1}, which is associated with the N—H wagging vibration of the amine group. These results verify that GO was functionalized with diamines. The typical peaks of β-CD are observed at 3352, 2932 and 1034 cm^{-1}, corresponding to the —OH stretching vibration, the $—CH_2$ asymmetric stretching vibration and the C—O—C stretching vibration,

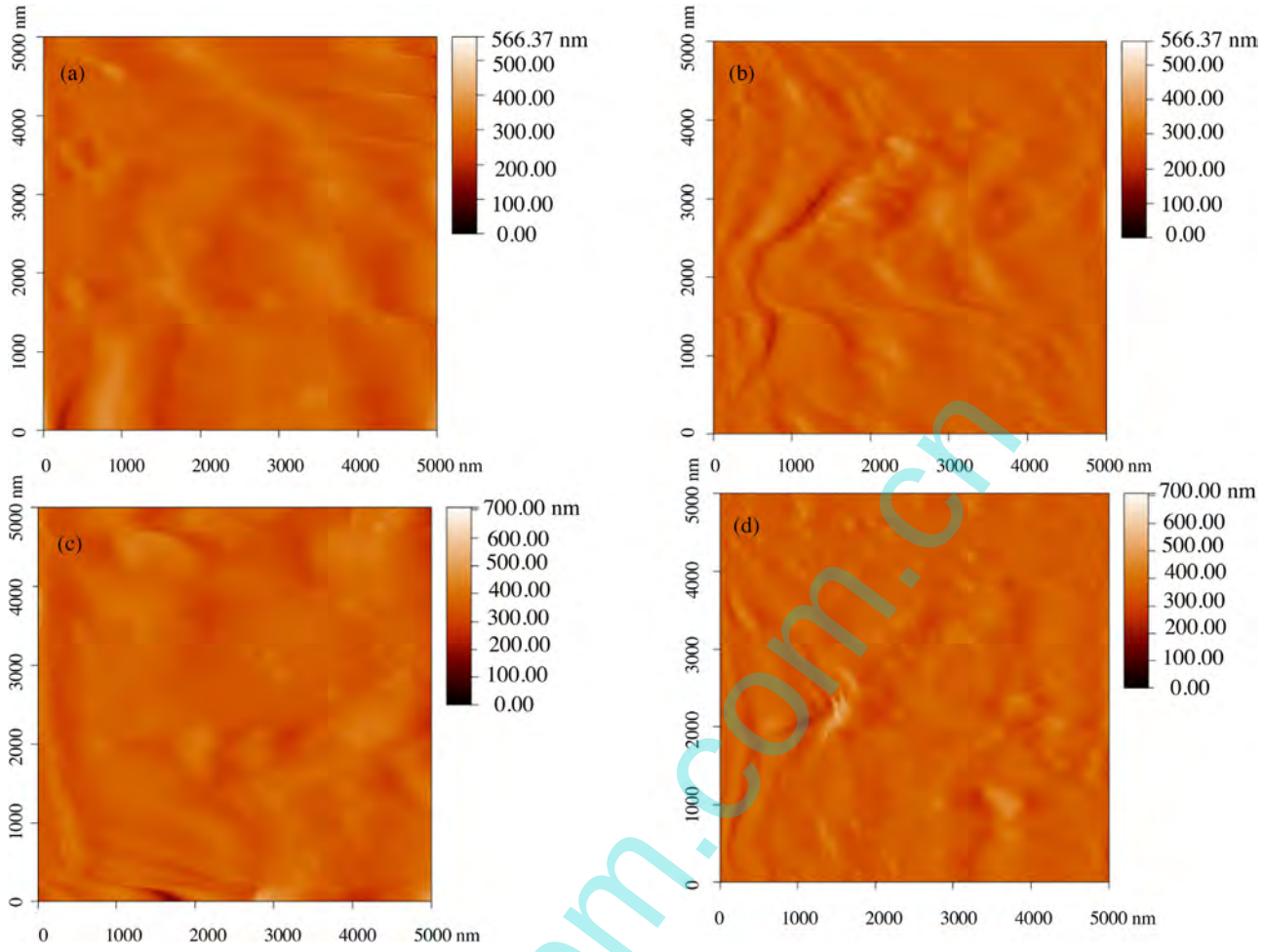

Fig. 3. AFM images of (a) GO; (b) EA-GO; (c) HA-GO and (d) β-CD-GO thin films.

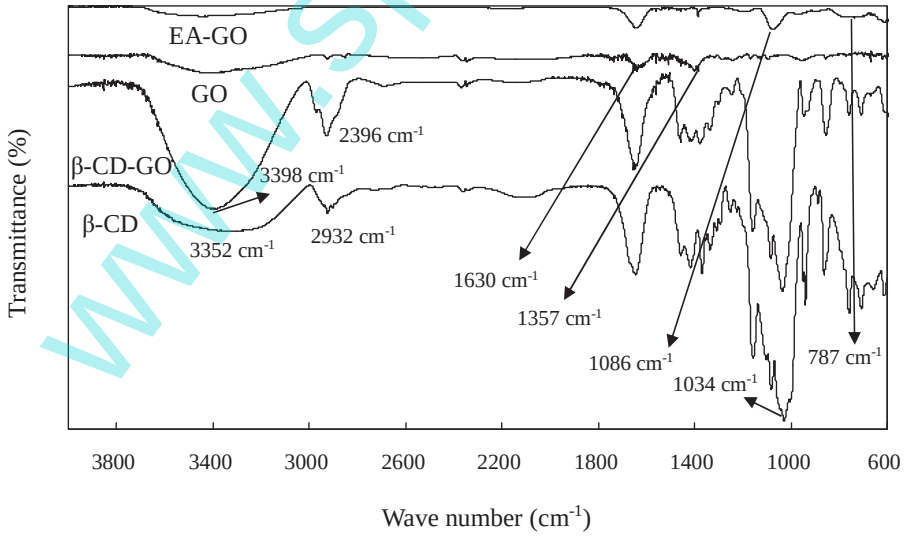

Fig. 4. IR spectra of GO, EA-GO and β-CD-GO thin films.

respectively. Decorating the GO with β-CD shifted the peak (from β-CD) at 3352 cm^{-1}, which corresponds to the —OH stretching vibration, to 3398 cm^{-1} (from β-CD-GO), because hydrogen interactions between the hydroxyl groups of β-CD and some of the oxygen groups of GO resulted in hydrogen bonding. These results verify that GO was functionalized with β-CD.

www.spm.com.cn

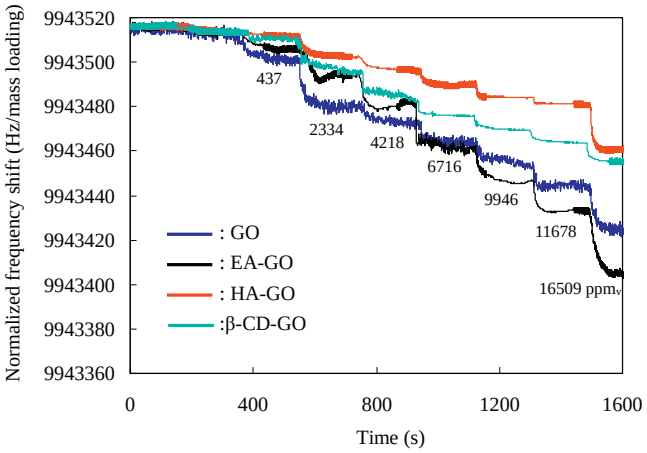

Fig. 5. Normalized frequency shifts (Hz/μg) as a function of time (s) for different volume ratio of the moist air on GO, EA-GO, HA-GO and β-CD-GO thin films.

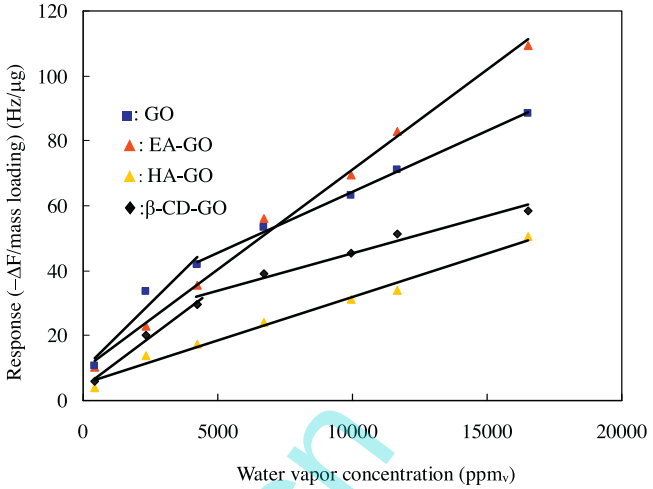

Fig. 6. Response (−ΔHz/μg) as a function of volume ratio (ppm$_v$) for GO, EA-GO, HA-GO and β-CD-GO thin films.

Table 1
Sensitivity to humidity of GO, EA-GO, HA-GO and β-CD-GO thin films that were coated on QCM for different volume ratios of moist air.

	Sensitivity[a]			
Δppm$_v$[b]	GO	EA-GO	HA-GO	β-CD-GO
437	0.0343	0.0312	0.0091	0.0204
2334	0.0198	0.0131	0.0059	0.0127
4218	0.0137	0.0114	0.0040	0.0105
6716	0.0110	0.0113	0.0035	0.0087
9946	0.0087	0.0094	0.0031	0.0068
11678	0.0084	0.0095	0.0028	0.0065
16509	0.0074	0.0089	0.0030	0.0052

[a] The sensitivity of the various sensing films was defined as $\frac{-\Delta Hz}{\Delta ppm_v \times \mu g}$.

[b] The Δppm$_v$ was defined as the volume ratio subtracted by the initial volume ratio of moisture air (2.77 ppm$_v$).

Table 2
Linear sensing characteristics of GO, EA-GO, HA-GO and β-CD-GO thin films that were coated on QCM at different volume ratio of moist air.

	Sensing characteristics					
	437–4218 ppm$_v$		6716–16509 ppm$_v$		437–16509 ppm$_v$	
	Slope	Linearity[a]	Slope	Linearity[a]	Slope	Linearity[a]
GO	0.0082	0.9344	0.0037	0.9961	0.0044	0.9576
EA-GO	0.0067	0.9998	0.0055	0.9920	0.0062	0.9945
HA-GO	0.0035	0.9242	0.0020	0.9799	0.0027	0.9851
β-CD-GO	0.0063	0.9896	0.0027	0.9782	0.0031	0.9259

[a] The linearity was defined as the linear regression coefficient of R^2-value of linear fitting curve.

3.3. *Low-humidity sensing properties of GO, EA-GO, HA-GO and β-CD-GO thin films*

Fig. 5 plots the frequency shifts of GO, EA-GO, HA-GO and β-CD-GO thin films as functions of time for various volume ratios of moist air in the range of 437–16,509 ppm$_v$. The frequency shifts of the GO, EA-GO, HA-GO and β-CD-GO thin films were normalized to the mass of the coated sensing materials. Table 1 lists the corresponding sensitivities of the GO, EA-GO, HA-GO and β-CD-GO thin films. Fig. 6 plots the results of calibration curves of GO, EA-GO, HA-GO and β-CD-GO thin films and Table 2 presents their slope and linear correlation coefficient (R^2). When the volume ratio of moist air was 437 ppm$_v$, the sensitivities of GO, EA-GO, HA-GO and β-CD-GO thin films were 0.0343, 0.0312, 0.0091 and 0.0204, respectively (Table 1). At low humidity (<6716 ppm$_v$), the normalized frequency shifts followed the order HA-GO < β-CD-GO < EA-GO < GO (Fig. 5). However, when the volume ratio of moist air exceeded 6716 ppm$_v$, the sensitivity of the EA-GO thin film was higher than that of the GO thin film. The linear sensing characteristics of both GO and β-CD-GO thin film in the range 473–4218 differed from those in the range 6716–16,509 ppm$_v$. The slope declined steeply as the volume ratio of moist air increased from 6716 to 16,509 ppm$_v$ (Fig. 6 and Table 2). Additionally, the normalized frequency shift of the EA-GO thin film increased steeply with the volume ratio of moist air above 6716 ppm$_v$ (Fig. 5). Therefore, the sensitivity of the EA-GO thin film to humidity and the linearity of its adsorption were better than those of the functionalized-GO thin films over a wide range of humidities, 4713–16,509 ppm$_v$ (Fig. 6 and Table 2). The GO thin film was further tested for evaluation of humidity of detection limit (D.L.) because it exhibited highest frequency shifts. The D.L. was defined as the signal-to-noise ration equal to 3 ($S/N = 3$) and calculated to be 116 ppm$_v$. Moreover, the stability test, where the GO, EA-GO, HA-GO and β-CD-GO thin films were subjected to repeated humidification and desiccation cycles more than 50 times in the range 473–4218 ppm$_v$, indicated that the GO, diamine-functionalized GO and β-CD-functionalized GO thin films worked normally during the test.

As described in Section 3.1, the EA-GO, HA-GO and β-CD-GO thin films had rougher surfaces than the GO thin film and they did not vary significantly in surface roughness. Therefore, the response of the functionalized-graphenes thin films to humidity, especially at low levels, was not related to surface morphology. This finding can be understood by considering that —COOH, —$CONHC_2H_4NH_2$, —$CONH(C_2H_4)_3NH_2$ and β-CD functional groups on the surface of graphene influence the low-humidity sensing properties of the material. The GO film (with the —COOH functional group) adsorbed the most water molecules because water vapor was preferentially adsorbed on polar oxygen-containing defects (COOH) by the formation of hydrogen (H) bonds [34–36]. Water molecules were more easily adsorbed onto the EA-GO film (with the —$CONHC_2H_4NH_2$ functional group) than on the HA-GO film (with the —$CONH(C_2H_4)_3NH_2$ functional group) because HA has a longer alkyl chain than does EA, so its adsorption by hydrogen bond is inferior, causing the EA-GO film to be more sensitive. Water molecules were adsorbed as stable host–guest inclusion complexes onto the β-CD cavities of the β-CD-GO thin film. At a higher volume ratio of moist air (6716–16,509 ppm$_v$), fewer active sites are available for this reaction to occur, so the slopes of the curves for the GO and β-CD-GO thin films were highly negative. The EA-GO thin film was thicker and had a rougher surface than the GO film.

www.sp...n.cn

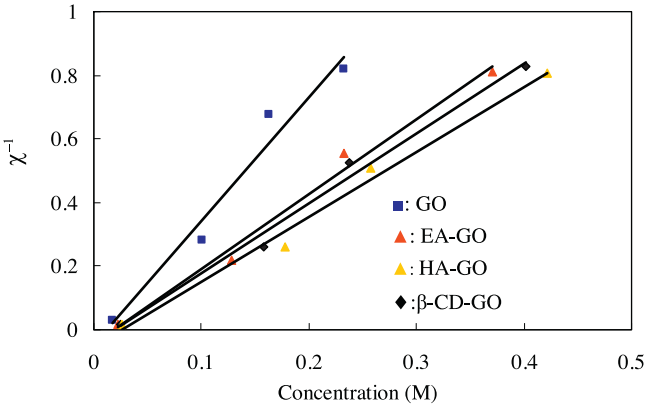

Fig. 7. Linear plot of the reciprocal of relaxation time (χ^{-1}) against vapor concentration (M) for GO, EA-GO, HA-GO and β-CD-GO thin films.

Many water vapor molecules accumulated around the pores, facilitating capillary condensation, so the sensitivity of the EA-GO thin film exceeded that of the GO thin film when the volume ratio of moist air exceeded 6716 ppm_v (Figs. 5 and 6).

3.4. Adsorption properties of GO, EA-GO, HA-GO and β-CD-GO thin films

To elucidate the low-humidity sensing properties of the functionalized GO thin films, especially at low humidity (<6716 ppm_v) (Fig. 5), the dynamics of adsorption of water molecules onto GO, EA-GO, HA-GO and β-CD-GO thin films that were coated on QCM were studied. The following reaction explains the adsorption behaviors of water molecules onto GO, EA-GO, HA-GO and β-CD-GO thin films [23,37]. The time course of adsorption at the experimental dilute concentration is expressed simply as the follows.

$$\text{Sensing films} + \text{water vapour molecules} \underset{k_{-1}}{\overset{k_1}{\Leftrightarrow}} \text{Sensing films} - \text{water vapour molecules} \quad (3)$$

where k_1 and k_{-1} are the adsorption and desorption rate constants, respectively. The following equations give the amount of water vapor molecules, Δm_t, that are formed on the sensing films at time t under Langmuir isotherm adsorption conditions [23,37].

$$\Delta m_t = [\text{sensing films} - \text{water vapor molecules}]_t = \Delta m_\infty \left[1 - \exp\left(\frac{-t}{X}\right)\right] \quad (4)$$

$$X^{-1} = k_1 [\text{water vapor molecules}] + k_{-1} \quad (5)$$

where Δm_∞ is the maximal amount of water vapor molecules that are adsorbed on the sensing films at $t \to \infty$ and χ is the relaxation time. Adsorption time courses at various concentrations (0.0173–0.4213 M) are derived from Eqs. (4) and (5). Fig. 7 plots the linear correlation between the reciprocal of relaxation time (χ^{-1}) of adsorption and the concentration of water vapor on the sensing films (GO, EA-GO, HA-GO and β-CD-GO). Fig. 7 and Eq. (5) yield the adsorption rate constant k_1, the desorption rate constant k_{-1} and the association constant $K = (k_1/k_{-1})$ for water vapor on the sensing films (Table 3). The adsorption rate constant (k_1) of the functionalized-GO—water molecules decreased in the order GO > EA-GO > β-CD-GO > HA-GO. This experimental result reveals that water molecules are adsorbed more easily on GO than on EA-GO, β-CD-GO and HA-GO thin films, especially at low humidity (<6716 ppm_v) (Fig. 5). The GO thin film had a larger association constant K (70.05 M^{-1}) than EA-GO (53.45 M^{-1}), β-CD-GO (51.12 M^{-1}) and HA-GO (38.54 M^{-1}) thin films because the GO thin film had the highest adsorption rate constant (k_1). The variation in the association constants K among the GO, EA-GO and HA-GO thin films is explained by the variation in the stability of the hydrogen bond. Water molecules were adsorbed by the formation of hydrogen bonds more strongly on the GO thin film than on the diamines-functionalized GO thin films (EA-GO and HA-GO) because long alkyl chains made the hydrogen bonds weaker. The β-CD-GO thin film had smaller association constant K than the GO thin film, which finding is consistent with the experimental result that water molecules were less able to be adsorbed onto the β-CD-GO thin film than onto the GO thin film. These results reveal that the adsorption of water molecules onto GO, EA-GO, HA-GO and β-CD-GO thin films by the formation of hydrogen bonds has a predominant role in their sensing of low humidity. The GO thin film was more sensitive to water molecules than were the EA-GO, HA-GO and β-CD-GO thin films at low humidity (Table 1).

Table 3
Kinetic parameters for adsorption and desorption of water vapor molecules onto GO, EA-GO, HA-GO and β-CD-GO thin films.

Thin films	Adsorption rate constant, k_1 ($M^{-1}\,s^{-1}$)	Desorption rate constant, k_{-1} (s^{-1})	Association constant, K (M^{-1})
GO	3.923	0.056	70.05
EA-GO	2.352	0.044	53.45
HA-GO	2.043	0.053	38.54
β-CD-GO	2.198	0.043	51.12

4. Conclusions

Surface functionalization of GO can modulate its surface properties and sensitivity to low humidity. A GO thin film with a —COOH functional group was found to be effective for sensing low humidity (<6716 ppm_v). A GO thin film with a $-CONHC_2H_4NH_2$ functional group (EA-GO) exhibited the strongest sensitivity to water molecules (slope = 0.0062 Hz/μg ppm_v) and best linearity (R^2 = 0.9945), among those considered herein, over a wide range of humidities from 4713 to 16,509 ppm_v.

An adsorption dynamic analysis and molecular mechanical calculations revealed that the association constants K for water molecules onto functionalized GO thin films followed the order GO > EA-GO > β-CD-GO > HA-GO which is consistent with the experimental results herein. The large variation in the association constants K between the water molecules and the functionalized GO thin films arises from the predominance of adsorption by the formation of hydrogen bonds, especially at low humidity.

Acknowledgement

The authors thank the Ministry of Science and Technology (grant no. MOST 104-2113-M-034-001) of Taiwan for support.

References

[1] K.S. Novoselov, A.K. Geim, S.V. Morozov, D. Jiang, Y. Zhang, S.V. Dubonos, I.V. Grigorieva, A.A. Firsov, Electric field effect in atomically thin carbon films, Science 306 (2004) 666–669.
[2] K.S. Novoselov, A.K. Geim, S.V. Morozov, D. Jiang, M.I. Katsnelson, I.V. Grigorieva, S.V. Dubonos, A.A. Firsov, Two-dimensional gas of massless Dirac fermions in graphene, Nature 438 (2005) 197–200.
[3] A.A. Balandin, S. Ghosh, W. Bao, I. Calizo, D. Teweldebrhan, F. Miao, C.N. Lau, Superior thermal conductivity of single-layer graphene, Nano Lett. 8 (2008) 902–907.
[4] A. Lerf, H. He, M. Forster, J. Kilnowski, Structure of graphite oxide revisited, J. Phys. Chem. B 102 (1998) 4477–4482.

www.spm.com.cn

[5] J.L. Yan, G.J. Chen, J. Cao, W. Yang, B.H. Xie, M.B. Yang, Functionalized graphene oxide with ethylenediamine and 1,6-hexanediamine, New Carbon Mater. 27 (2012) 370–376.
[6] A.M. Shanmugharaj, J.H. Yoon, W.J. Yang, S.H. Ryu, Synthesis, characterization, and surface wettability properties of amine functionalized graphene oxide films with varying amine chain lengths, J. Colloid Interface Sci. 401 (2013) 148–154.
[7] V. Singh, D. Joung, L. Zhai, S. Das, S.I. Khondaker, S. Seal, Graphene based materials: past, present and future, Prog. Mater. Sci. 56 (2011) 1178–1271.
[8] T. Kuila, S. Bose, A.K. Mishra, P. Khanra, N.H. Kim, J.H. Lee, Chemical functionalization of graphene and its applications, Prog. Mater. Sci. 57 (2012) 1061–1105.
[9] P.G. Su, Z.M. Lu, Flexibility and electrical and humidity-sensing properties of diamine-functionalized graphene oxide films, Sens. Actuators B 211 (2015) 157–163.
[10] M.V. Rekharsky, Y. Inoue, Complexation thermodynamics of cyclodextrins, Chem. Rev. 98 (1998) 1875–1918.
[11] D.B. Lu, S.X. Lin, L.T. Wang, X.Z. Shi, C.M. Wang, Y. Zhang, Synthesis of cyclodextrin-reduced graphene oxide hybrid nanosheets for sensitivity enhanced electrochemical determination of diethylstilbestrol, Electrochim. Acta 85 (2012) 131–138.
[12] X.Q. Tian, C.M. Cheng, H.Y. Yuan, J. Du, D. Xiao, S.P. Xie, M.M.F. Choi, Simultaneous determination of L-ascorbic acid, dopamine and uric acid with gold nanoparticles-β-cyclodextrin-graphene-modified electrode by square wave voltammetry, Talanta 93 (2012) 79–85.
[13] M. Chen, Y. Meng, W. Zhang, J. Zhou, J. Xie, G. Diao, β-Cyclodextrin polymer functionalized reduced-graphene oxide: application for electrochemical determination imidacloprid, Electrochim. Acta 108 (2013) 1–9.
[14] P.R. Story, D.W. Galipeau, R.D. Mileham, A study of low-cost sensors for measuring low relative humidity, Sens. Actuators B 24–25 (1995) 681–685.
[15] Y. Sakai, Y. Sadaoka, M. Matsuguchi, Humidity sensors based on polymer thin films, Sens. Actuators B 35–36 (1996) 85–90.
[16] S. Zhang, Y. Zhu, S. Krishnaswamy, Nanofilm-coated photonic crystal fiber long-period gratings with modal transition for high chemical sensitivity and selectivity, Proc. SPIE 8346 (2012) 83460D.
[17] S. Zhang, Y. Zhu, S. Krishnaswamy, Fiber humidity sensors with high sensitivity and selectivity based on interior nanofilm-coated photonic crystal fiber long-period gratings, Sens. Actuators B 176 (2013) 264–274.
[18] R. Gao, D.F. Lu, J. Cheng, Y. Jiang, L. Jiang, Z.M. Qi, Humidity sensor based on power leakage at resonance wavelengths of a hollow core fiber coated with reduced graphene oxide, Sens. Actuators B 222 (2016) 618–624.
[19] A. Star, T.-R. Han, V. Joshi, J.R. Stetter, Sensing with Nafion coated carbon nanotube field-effect transistors, Electroanalysis 16 (2004) 108–112.
[20] M. Penza, G. Cassano, Relative humidity sensing by PVA-coated dual resonator SAW oscillator, Sens. Actuators B 68 (2000) 300–306.
[21] M. Neshkova, R. Petrova, V. Petrov, Piezoelectric quartz crystal humidity sensor using chemically modified nitrated polystyrene as water sorbing coating, Anal. Chim. Acta 332 (1996) 93–103.
[22] F.P. Delannoy, B. Sorli, A. Boyer, Quartz crystal microbalance (QCM) used as humidity sensor, Sens. Actuators A 84 (2000) 285–291.
[23] L.X. Sun, T. Okada, Simultaneous determination of the concentration of methanol and relative humidity based on a single Nafion(Ag)-coated quartz crystal microbalance, Anal. Chim. Acta 421 (2000) 83–92.
[24] A.J. Cunningham, Introduction to Bioanalytical Sensors, Wiley, New York, 1998, pp. 307.
[25] P.G. Su, Y.L. Sun, C.C. Lin, Novel low humidity sensor made of TiO_2 nanowires/poly(2-acrylamido-2-methylpropane sulfonate) composite material film combined with quartz crystal microbalance, Talanta 69 (2006) 946–951.
[26] P.G. Su, Y.P. Chang, Low-humidity sensor based on a quartz-crystal microbalance coated with polypyrrole/Ag/TiO_2 nanoparticles composite thin films, Sens. Actuators B 129 (2008) 915–920.
[27] H.W. Chen, R.J. Wu, K.H. Chan, Y.L. Sun, P.G. Su, The application of CNT/Nafion composite material to low humidity sensing measurement, Sens. Actuators B 104 (2005) 80–84.
[28] P.G. Su, Y.L. Sun, C.C. Lin, A low humidity sensor made of quartz microbalance coated with multi-walled carbon nanotubes/Nafion composite material films, Sens. Actuators B 115 (2006) 338–343.
[29] H.W. Chen, R.J. Wu, K.H. Chan, Y.L. Sun, P.G. Su, The application of CNT/Nafion composite material to low humidity sensing measurement, Sens. Actuators B 104 (2005) 80–84.
[30] P.G. Su, Y.L. Sun, C.C. Lin, A low humidity sensor made of quartz microbalance coated with multi-walled carbon nanotubes/Nafion composite material films, Sens. Actuators B 115 (2006) 338–343.
[31] P.G. Su, X.R. Kuo, Low-humidity sensing properties of carboxylic acid functionalized carbon nanomaterials measured by a quartz crystal microbalance, Sens. Actuators A 205 (2014) 126–132.
[32] P.G. Su, H.C. Shieh, Flexible NO_2 sensors fabricated by layer-by-layer covalent anchoring and *in-situ* reduction of graphene oxide, Sens. Actuators B 190 (2014) 865–872.
[33] G. Sauerbrey, The use of quartz oscillators for weighing thin layers and for microweighing, Z. Phys. 155 (1959) 206–222.
[34] Y. Yao, X. Chen, H. Guo, Z. Wu, Graphene oxide thin film coated quartz crystal microbalance for humidity detection, Appl. Surf. Sci. 257 (2011) 7778–7782.
[35] P.C.P. Watts, N. Mureau, Z. Tang, Y. Miyajima, J.D. Carey, S.R.P. Silva, The importance of oxygen-containing defects on carbon nanotubes for the detection of polar and non-polar vapors through hydrogen bond formation, Nanotechnology 18 (2007) 175701–175706.
[36] J.A. Robinson, E.S. Snow, S.C. Bădescu, T.L. Reinecke, F.K. Perkins, Role of defects in single-walled carbon nanotube chemical sensors, Nano Lett. 6 (2006) 1747–1751.
[37] Y. Okahata, M. Kawase, K. Niikura, F. Ohtake, H. Furusawa, Y. Ebara, Kinetic measurements of DNA hybridization on an oligonucleotide-immobilized 27-MHz quartz crystal microbalance, Anal. Chem. 70 (1998) 1288–1296.

Biographies

Pi-Guey Su is currently a professor in Department of Chemistry at Chinese Culture University. He received his BS degree from Soochow University in Chemistry in 1993 and Ph.D. degree in chemistry from National Tsing Hua University in 1998. He worked as a researcher in Industrial Technology Research Institute, Taiwan, from 1998 to 2002. He joined as an assistant professor in the General Education Center, Chungchou Institute of Technology from 2003 to 2005. He worked as an assistant professor in Department of Chemistry at Chinese Culture University from 2005 to 2007. He worked as an associate professor in Department of Chemistry at Chinese Culture University from 2007 to 2010. His fields of interests are chemical sensors, gas and humidity sensing materials and humidity standard technology.

Yu-Te Lin received a B.S. degree in Environmental Engineering from Da Yeh University in 2012. He entered the MS course of Chemistry at Chinese Culture University in 2014. His main areas of interest are humidity-sensing materials.

www.spm.com.cn